Proceedings of ASME Turbo Expo 2011
GT2011
June 6-10, 2011, Vancouver, British Columbia, Canada

GT2011-46391

SUB-MINIATURE FIVE-HOLE PROBE CALIBRATION USING A TIME EFFICIENT PITCH AND YAW MECHANISM AND ACCURACY IMPROVEMENTS

Jason Town[1]
Turbomachinery Aero-heat Transfer Laboratory
Department of Aerospace Engineering
The Pennsylvania State University
University Park, Pennsylvania 16802
Email: jet234@psu.edu

Cengiz Camci[2]
Turbomachinery Aero-heat Transfer Laboratory
Department of Aerospace Engineering
The Pennsylvania State University
University Park, Pennsylvania 16802
Email: cxc11@psu.edu

ABSTRACT

A five-hole probe is a proven aerodynamic tool for the accurate measurement of flow fields, but is traditionally difficult to calibrate manually in an acceptable range of pitch and yaw angles. With advancements in computer technology, it is possible to improve the calibration process that is made up of tedious and repeating angular pitch and yaw angle movements. This paper proposes a way to increase the accuracy of measurements. The proposed approach uses computer automation, a mechanical pressure scanner, and precision rotary tables to significantly reduce the amount of time required to complete the calibration sequence. A five-hole probe is fastened to a precision calibration mechanism in a wind tunnel test section. This mechanism varied the pitch and yaw angle of the probe accurately via two computer controlled rotary tables. This approach allowed for a much greater degree of accuracy and a way to increase the number of data points taken, better defining the non-linear portions of the calibration maps. The scanivalve system minimized the number of transducers required from seven to one. While it takes more time than having multiple transducers, this approach lowered the overall equipment costs and helped to reduce measurement errors. The data acquisition device provides an interface between the rotary table stepper controllers, the scanivalve controller, and the transducer. A LabVIEW interface was then used to control all of the devices, while simultaneously retrieving data from the transducer and turning it into the coefficients needed to make the calibration map. The program allows for a degree of flexibility, allowing the user to choose the range of angles and the degrees between each point.

INTRODUCTION

Five-hole probes are used to determine all three components of the mean velocity vector, Wiedner [1]. They work by selectively comparing pressure data from five ports on the probe. According to Treaster and Yocum [2], by comparing the pressure differences between these ports, flow velocity, pitch angle, yaw angle, total pressure and static pressure can simultaneously be determined. However, this was found to work only in a range of ±30° pitch and yaw angle. To increase this range, a method of nulling the yaw ports was suggested by Ostowari and Wentz [3]. This method increases the range to ±85°, but it is not always possible to null the yaw ports, especially in internal flows such as that of a turbine. Nowack [4] attempts to increase the range at which a five-hole probe may be used by developing a long, spherical probe. While this probe brought the usable range up to ±65°, the size of the probe makes it hard to incorporate in many cases.

Interpolation to find the necessary coefficients has been accomplished through a variety of methods. One of the original ways was to use curve fitting approach used by Treaster and Yocum [2] and Weiz [5]. Reichert and Wendt [6] suggested another method to reduce the data. This method replaces the pitch and yaw angles with unit vectors and developed a Taylor series based approach to use instead of linear interpolation.

Dominy and Hodson [7] have studied the effects of Reynolds number extensively. These studies show how probe design can affect how Reynolds number creates error. Treaster and Yocum [2], who suggested that the map be made at the same Reynolds number that is expected or a correction factor be used, also examined this previously. Morrison, Schobeiri, and Pappu [8]

[1] Graduate Research Assistant
[2] Professor of Aerospace Engineering

proposed a method for the detection of abnormalities in the probe. This aids in the identification of probe damage and flow alignment issues.

Investigations into the effects of near-wall measurements by Treaster and Yocum [2] and Lee and Yoon [9] have concluded that measurements should be taken from a distance of at least twice the probe diameter from a wall. If it is necessary to operate closer than this distance, Lee and Yoon [9] provide a guideline to make such measurements.

Brophy et al. [10] suggested five-hole probes might also be used in place of laser Doppler anemometers for wake measurements. The main application of such a probe would be in locations where it would be difficult to use a laser, such as the rotating frame of reference in a turbine research rig. Thus, Sitaram, Lakshminarayana, and Ravindranath [11] performed a study on which type of probe to use within this frame of reference at the Pennsylvania State University.

NOMENCLATURE

$C_{P_{yaw}}$ – Non-dimensionalized value of yaw pressure
$C_{P_{pitch}}$ – Non-dimensionalized value of pitch pressure
$C_{P_{total}}$ – Non-dimensionalized value of total pressure
$C_{P_{static}}$ – Non-dimensionalized value of static pressure
P_1 – Pressure point 1, as defined in Figure 1
P_2 – Pressure point 2, as defined in Figure 1
P_3 – Pressure point 3, as defined in Figure 1
P_4 – Pressure point 4, as defined in Figure 1
P_5 – Pressure point 5, as defined in Figure 1
$\bar{P}$ – Average value of outside pressure points
α – Pitch angle
β – Yaw angle
P – Atmospheric Pressure
ρ – Density
P_T – Total pressure
P_S – Static pressure
V – Absolute velocity
u – Velocity component in the x-direction
v – Velocity component in the y-direction
w – Velocity component in the z-direction
V_1 – Voltage as measured at point 1, as defined in Figure 1
V_2 – Voltage as measured at point 2, as defined in Figure 1
V_3 – Voltage as measured at point 3, as defined in Figure 1
V_4 – Voltage as measured at point 4, as defined in Figure 1
V_5 – Voltage as measured at point 5, as defined in Figure 1
V_T – Voltage as measured at the total pressure port
V_S – Voltage as measured at static pressure port
z – Zero voltage measurement
c – Calibration constant
δP_i –Relative error

CALIBRATION TECHNIQUE

A modified version of the calibration technique of a non-nulling five-hole probe used by Treaster and Yocum is used in this paper. The main difference between the techniques is in the way the pitch and yaw angles are defined. Figure 1 defines the position of the holes. The correct numbering was verified by blowing compressed air though each one of the five ports of the probe.

The five pressures that are obtained from the probe can then be non-dimensionalized as follows.

$$C_{P_{yaw}} = \frac{P_2 - P_3}{P_1 - \bar{P}} \quad (1)$$

$$C_{P_{pitch}} = \frac{P_5 - P_4}{P_1 - \bar{P}} \quad (2)$$

$$C_{P_{total}} = \frac{P_1 - P_{total}}{P_1 - \bar{P}} \quad (3)$$

$$C_{P_{static}} = \frac{\bar{P} - P_{static}}{P_1 - \bar{P}} \quad (4)$$

$$\bar{P} = \frac{P_2 + P_3 + P_4 + P_5}{4} \quad (5)$$

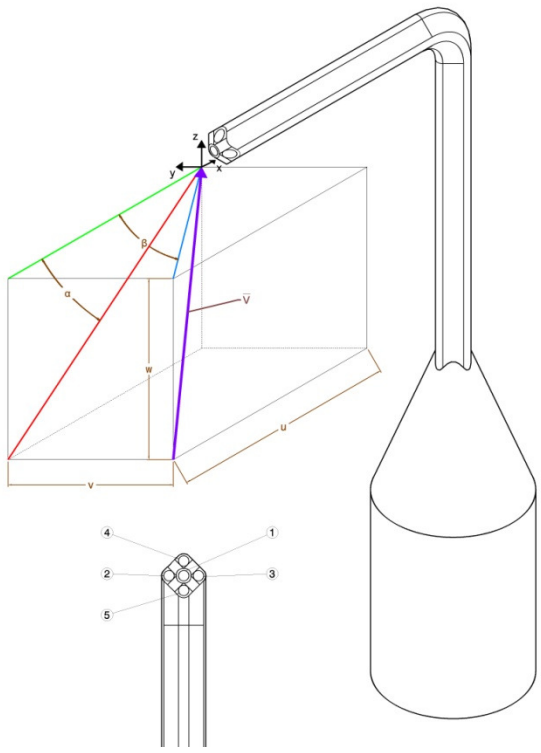

Figure 1: Isometric View of a Sub-Miniature Five-Hole Probe with Velocity Vector, Positive Angles, and Positive Velocity Components and Probe Port Number Assignments

In this configuration, if you were positioned behind the probe facing the incoming flow, the positive pitch would be when the flow is from below the probe (nose up). Positive yaw value would be when the flow is from the left. This can also be seen in Figure 1, where $\bar{V}$ is the velocity vector, $u\ v\ w$ are its components and all values are positive as shown in the figure.

CALIBRATION HARDWARE

The system used to gather calibration data is shown in Figure 2. This figure shows the major flow of data from and to the computer. All data must go through a 16-bit data acquisition system (DAQ), as it acts as interface for the computer. First, the DAQ instructs the stepper motors where to move to, via digital I/O ports, changing the pitch and yaw angle of the probe. The probe then provides five pressure measurements via the scanivalve a single variable reluctance transducer. The DAQ controls the scanivalve, selecting the pressure channel. The pressure is then sent to the transducer, which turns it into an analog signal. Finally, the DAQ reads the signal from the transducer, digitizes it, and sends it back to the computer to be recorded.

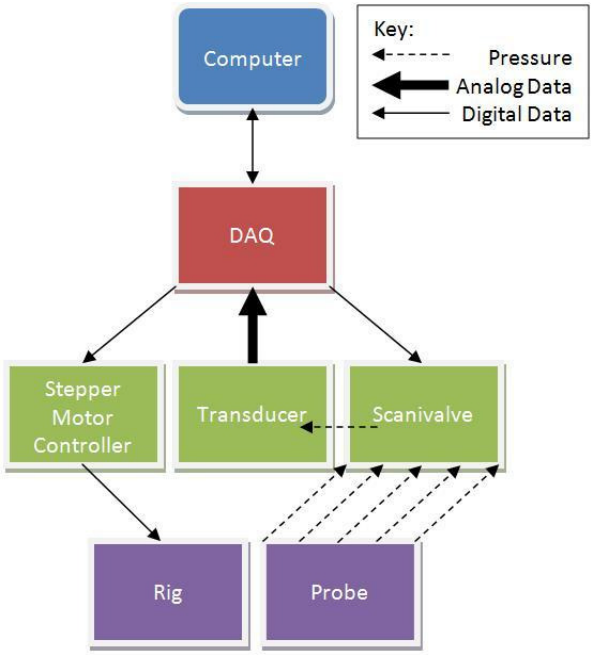

Figure 2: Major Component Block Diagram

Data Acquisition Device

A 16-bit DAQ made by Measurement Computing Corporation (model USB-1608FS) was used. It can obtain 200k samples per second over a Universal Serial Bus interface, and has an accuracy of ±0.68 mV at a range of ±1 V. This DAQ was chosen due to its 16-bit capabilities in order to help increase the accuracy of the measurements. With this, the pressure transducer output was directly interfaced to the DAQ without the need for further signal amplification. This is because of the 16-bit resolution of the A/D converter.

Scanivalve

A Scanivalve Corporation mechanical pressure selector with a controller and digital readout, model number CTLR2(P)/S2-S6, was used. This system can mechanically scan though a large number of pressure ports using a stepper motor-based selector system. The mechanical scanning approach reduced the number of transducers that was needed. The “step" and “home” commands needed for the operation of the scanner were provided by the digital output ports of the DAQ system. The mechanical scanning approach has its error reduction benefit since pressure differentials defined in the first five equations are always measured by one single transducer.

For Example, (P_5-P_4) is directly proportional to the pitch angle and is measured by separate measurements of P_5 and P_4 using the same transducer. The subtraction between P_5 and P_4 eliminates some of the error introduced by the single transducer. The mechanical scanning approach required for using a single transducer contributes to the error reduction during the construction of the calibration maps. This scanning also reduces the total cost of the transducers in this system. Although there is a significant calibration error reduction in the current mechanical scanning approach, the time required for the completion of the calibration maps is relatively increased. However, the fully computerized pitch and yaw movements in this current approach easily compensate for this time increase.

Transducer

A Validyne DP15 Low Pressure Transducer was used to measure pressures from the five ports of the probe. The reference side of the transducer was left open the atmosphere. The transducer itself was placed on a wooden board in an effort to help keep the air near it still. It was also placed as far as possible from any active electrical lines in order to keep down electrical interference and noise. It was used in conjunction with a Validyne Sine Wave Carrier Demodulator. DP15’s accuracy was rated as 0.25% of the full-scale measurement range that is ±3.5 Pascal with the selected diaphragm.

Stepper Motor Controllers

Two identical stepper motor controllers manufactured by Applied Motion Products were required for this setup. Via the DAQ, it is possible to control the direction and the number of steps to take in the selected direction. The drivers are never used simultaneously, as they share a single 24V, 5.0A power supply. The “step” and “change of direction” commands (TTL) are provided to the controllers via the digital I/O ports of the DAQ. All pitch and yaw angle related stepper motor control decisions are coordinated by a LabView graphical interface script.

Rotary Tables

Two rotary tables from Velmex Inc. were used to complete the pitch and yaw calibration rig. The first one is model B4800TS. It is the larger of the two, and is used to change the pitch angle

of the probe. It moves 0.025 degrees per step. The rotary table details are shown in Figure 3.

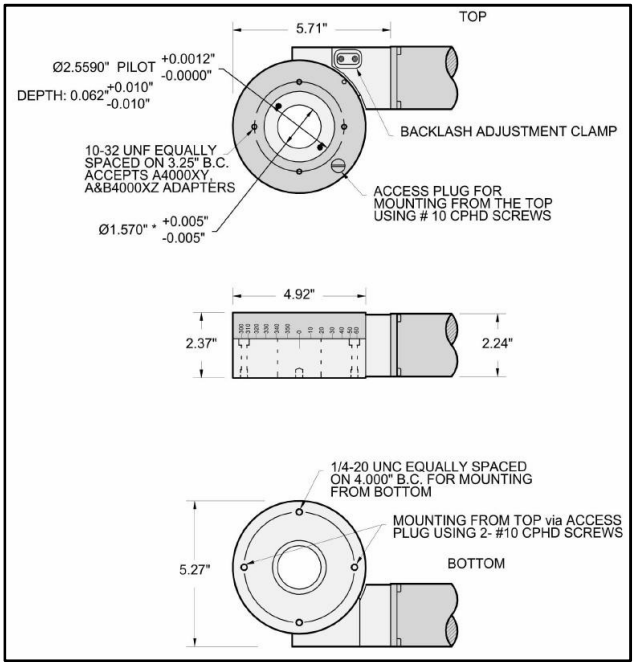

Figure 3: Rotary Table B4800TS

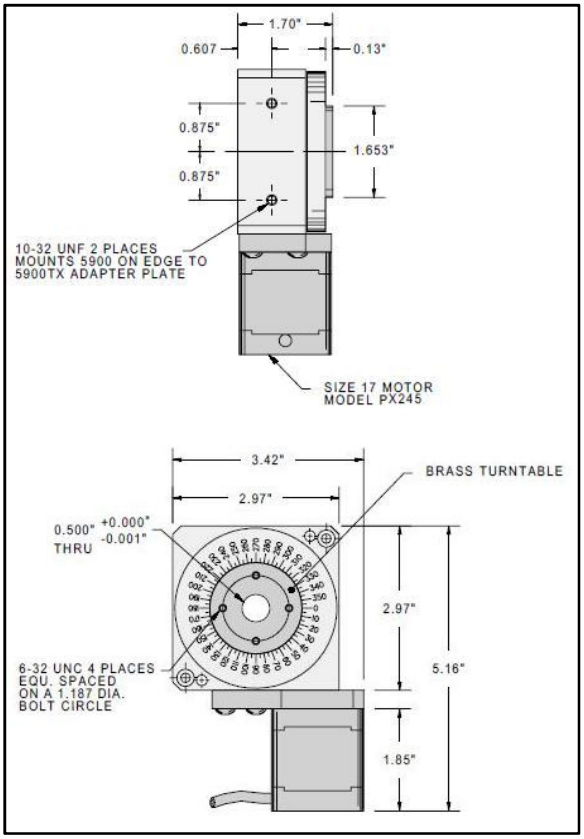

Figure 4: Rotary Table B5990TS

The second table is the B5990TS, and it is used for yaw adjustments. With each step, it moves 0.020 degrees. This rotary table was modified in order to allow an extension for a probe holder to fit through. Geometric details of this rotary table are shown in Figure 4.

Pitch and Yaw Calibration Rig

The original pitch and yaw calibration rig as shown in Figure 5, held the probe by the neck. The larger turntable (B4800TS) changed the yaw angle, and when the probe was at zero pitch, the axis of the yaw table and the probe coincided. The smaller turntable (B5900TS) changed pitch (stem) angle. In Figure 5, the axes of rotation are represented by red dashed centerlines. Since the tip of the probe was so far away from the pitch rotational axis the location of the probe tip would vary significantly in the direction along the probe stem. Since the measurements were taken in a free jet with a square cross section, there was a concern that axial decay, mixing turbulence, boundary layer effects, etc. could affect the calibration map. This was of most concern when the probe changed its angles to the extremes of the map because the relatively large arm of the probe stem would move the tip far from its starting position, the rotations are represented in Figure 5.

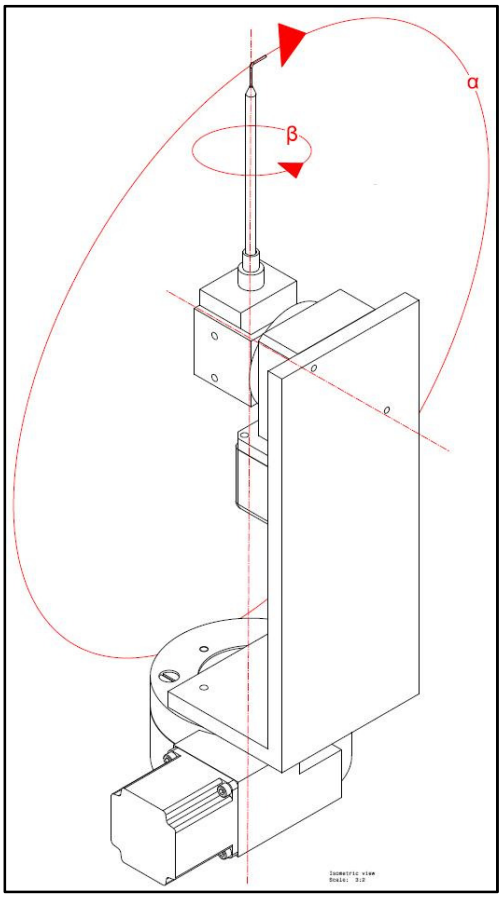

Figure 5: Original Rig Design

Improved Pitch and Yaw Calibration Rig

A new design was decided upon as shown in Figure 6. This rig changes the role of the turntables. Now, the larger turntable (B4800TS) changes the pitch, while the smaller turntable (5900TS) changes the yaw angle. The rotational axes are once again represented as red centerlines. The main advantage of this design was that the bend in the probe is now located at the intersection of the pitch and yaw axis. This approach greatly shortened the probe arm allowing the probe tip to stay well within the core flow. The movement of the probe tip in the new design is much smaller than the tip displacement of the original design.

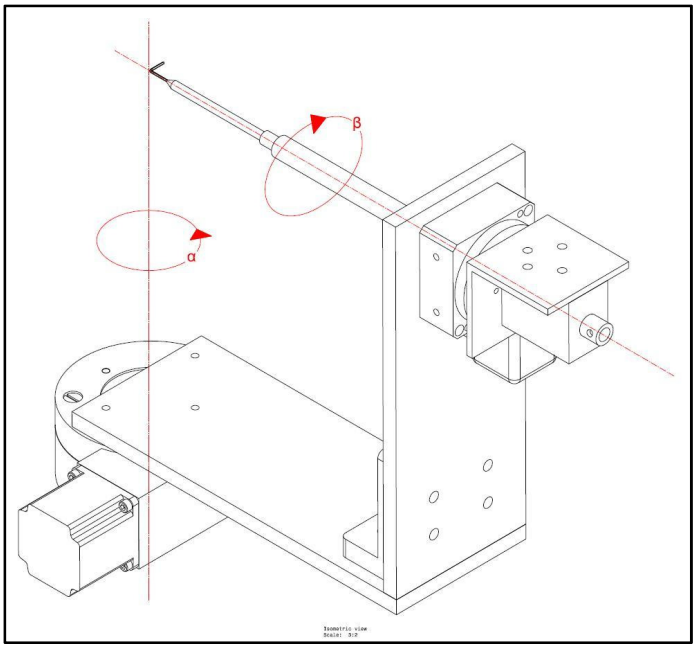

Figure 6: Calibration Rig

Probes

A sub-miniature five-hole probe was manufactured on site using five hypodermic needles. The five-hole probe as shown in Figure 1 has a square cross-section with one hole in the center surrounded by 4 more above, below, left and right of it. The tip has all but the center beveled to a 45° angle. The hypodermic needles are used to reduce the size of the probe have a maximum diameter of 1.68 mm at the tip, thus reducing the disturbance caused by it. A detailed description of the probe used in this study is also provided in Treaster and Houtz [12]. The small diameter hypodermic tubing used in the current sub-miniature probes inherently increased the waiting/sampling time needed to let the pressure transients settle in a connector tubing with a very large L/D ratio. Although the sub-miniature probe operation requires a longer sampling time, the small probe tip size increases the spatial resolution of our measurements greatly and allows the researcher to insert this probe into extremely complex internal flow areas in turbomachinery.

A simple Pitot probe was also used in the calibration wind tunnel test section as shown in Figure 7. The Pitot probe's response time was much faster than the five-hole probe. The tunnel total pressure, static pressure, and wind velocity at the five-hole probe tip location obtained from this reference Pitot probe are used for the calculations of the five non-dimensional coefficients for the calibration maps.

Wind Tunnel

The facility consisted of an open loop wind tunnel with an axial air blower, a diffused housing with multiple screens, a plenum chamber, a high area ratio circular nozzle, a circular to square transition nozzle, and a section of constant cross section duct. The motor was a constant speed motor and was rated at 7.5Kw. It drives a fan that is 45.7 cm tip to tip. The test was performed in the free stream just outside the end of the constant cross section duct as described in Figure 7. Figure 7 shows a drawing of the wind tunnel with pertinent dimensions. The test section velocity is continuously adjustable via an AC inverter connected to the motor. Turbulent flow characteristics in the test section could be adjusted to any turbulence intensity value between 0.5% and 1.2% by the use of calibrated screens and bi-plane turbulence promoters. Details of the test section flow quality can be found in Wiedner [1].

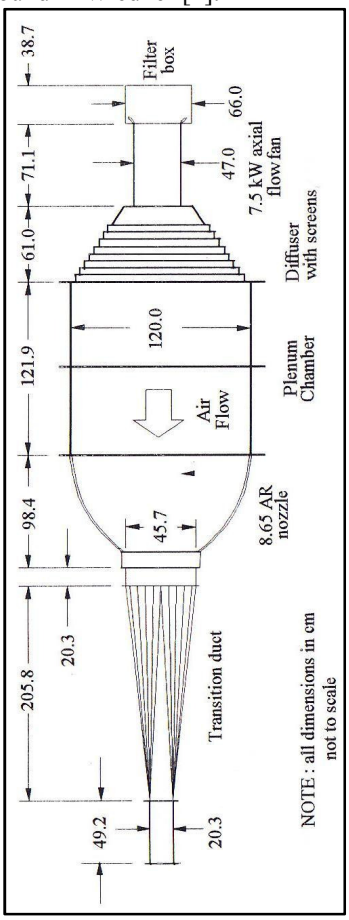

Figure 7: Wind Tunnel Dimensions

Graphical Interface

The graphical/analytical interface in the current calibration system was written as a LabVIEW code in two parts. One program was used to obtain the carpet map automatically and the other program was to take inputs and return values using the map.

Gathering Data for the Carpet Map

An automated program was written to perform a complete calibration without any human intervention. The only manual operator input into this calibration sequence is the initial hand positioning of the probe at the zero pitch, zero yaw angles. The program first prompts the user for a pitch and yaw range over which the measurements should be taken. Then the program asks what the angle increment between each measurement should be. For example, if you choose an overall range of ±30°, and an angular increment of 10°, then the program will make a seven by seven map with 49 points. It also asks the user how long and fast it should take data, and for a wait time between scanivalve moves. The flow of the program is as follows; first, the computer takes zero values of the pressure transducer output for each hole while the tunnel is not running. Next, it moves the probe to -30° yaw, -30° pitch. From there the user is prompted to start the calibration by the Labview interface. This is to allow time for the wind tunnel to reach its steady maximum speed. It varies the pitch for constant values of yaw, and records all the data into a matrix. Finally, when all the data is collected, the program calculates the requested non-dimensional coefficients by using the values from the aforementioned data matrix and applying them to Equation 1 through Equation 5.

Using the Carpet Map to Find Pitch and Yaw

A FORTRAN code recently developed in-house was used as baseline during the development of the new LabVIEW code. This code was consistently used in the manual five-hole probe calibration procedure previously performed in our laboratory. The recent fully automated LabVIEW implementation of the same analytical calibration/reduction procedure was shown to produce identical results when compared to our past manual calibration/reduction system.

The code works by the user inputting the current temperature and atmospheric pressure (P). With these values it is possible to find density (ρ) from the equation of state. The program also requires a calibration factor documenting how many volts of "Validyne pressure transducer output" per inch of water column as applied pressure. Next, the computer program takes the current voltage that was measured, and subtracts the calibration zeros that were measured before. This is to help reduce pressure measurement error due to thermal drift of the transducer output. Subsequently it calculates the values of $C_{p_{yaw}}$, $C_{p_{pitch}}$ and $\bar{P}$ using Equation 1, Equation 2, and Equation 5, respectively.

The program then determines the pitch angle α. This is found by a series of linear interpolations. The first set is done by taking a set of $C_{p_{yaw}}$ values from the map and separating them into constant pitch angles. By comparing them to the calculated $C_{p_{yaw}}$value, and finding the values of $C_{p_{pitch}}$. This leaves a 1-D array of $C_{p_{pitch}}$ values, which is as long as the matrix but only one dimension wide that are at constant $C_{p_{yaw}}$. Next, another linear interpolation is done, this time it uses the 1-D array of $C_{p_{pitch}}$ values that was just created, and compares it to the calculated $C_{p_{pitch}}$from Equation 2. The second matrix, which it is using to find the answer, is the range of α angles that the map spans.

Next, the pitch angle β is to be found. This is done in a similar fashion to the α angle results. Once again, a series of interpolations is performed in order to find an array. This time though, α, which was found just a moment ago, is held constant and the range which α spans is used. Using interpolation once again, a 1-D array of $C_{p_{yaw}}$ values is found. This array is compared to the calculated value of $C_{p_{yaw}}$ from Equation 1, and held up against the range that the β angle spans. This interpolation yields the β angle of the flow.

Afterward, α angle and the α array are once again used for interpolation. This time though, it is used to create a 1-D array of $C_{p_{total}}$ values. $C_{p_{total}}$values are then compared to the calculated β value and the β array in yet another interpolation. This results in a single value for $C_{p_{total}}$.

A final series of interpolations are performed, this approach once again uses a constant α angle and the α array. This time the interpolation yields a series of $C_{p_{static}}$ values. These values are used in conjunction with the constant β value and the range which β varies for a final interpolation. This gives the last coefficient function, which is the $C_{p_{static}}$ value.

With these values found, the following operations were performed. To find total and static pressure the following equations were used.

$$P_T = P_1 - C_{P_{total}}(P_1 - \bar{P}) \qquad (6)$$

$$P_S = \bar{P} - C_{P_{static}}(P_1 - \bar{P}) \qquad (7)$$

In Equation 6 and Equation 7, a conversion may be necessary to change the units of pressure.

Next, the magnitude of velocity vector of the flow was found using Bernoulli's equation for an incompressible flow from Equation 8.

$$V = \left[\frac{2(P_T - P_S)}{\rho}\right]^{\frac{1}{2}} \quad (8)$$

Since the angles are already known, it is possible to find the individual components of the velocity vector with a simple geometrical calculation derived from Figure 1. The velocity component calculations are as follows.

$$u = V\cos\beta\cos\alpha \quad (9)$$

$$v = V\sin\beta \quad (10)$$

$$w = V\sin\alpha\cos\beta \quad (11)$$

Finally a clause was put in so that if the α or β angle was found to be greater than 35°, the program would simply return zeros for all values as a cautionary flag.

CALIBRATION RESULTS AND DISCUSSION

Minimizing error

One of the main concerns with calibrating a five-hole probe is producing a high quality map with reduced absolute error. In theory, the map should look the same each time the probe is calibrated. This is hardly the case for there are many sources of error. One concern is changes in calibration flow quality that can be caused by laboratory disturbances or unwanted air currents during a calibration. Another source of error can occur when the probe is first aligned with the flow. The probe was initially aligned by hand and as such was prone to human error.

Thus, the best time to perform a test run seemed to be at night or when disturbances were minimal. Next, only one transducer was used to sample pressure from all seven-pressure measurement points. Five channels were required for the five-hole probe ports and two channels were needed for the simple Pitot probe documenting the tunnel velocity, total pressure and static pressure in the test section.

Using one single transducer for all seven measurements during calibration increased the elapsed time for a complete calibration. However, this approach helped to eliminate some of the calibration errors. The following evaluations can be done on Equation 1 through Equation 4.

$$P_n = (V_n - z)c \quad (12)$$

Equation 12 states that pressure is a function of the measured V_n, z, and c. Since the zero and the calibration factor exist only for one transducer, they can be considered constant for all pressure values. The next step will only take $C_{P_{Total}}$ from Equation 3 into consideration, though this can be done with any of the other pressure coefficient equations. By substituting Equation 12 into Equation 3, the following can be found.

$$C_{P_{Total}} = \frac{(V_1 - z)c - (V_T - z)c}{(V_1 - z)c - \frac{(V_2 - z)c + (V_3 - z)c + (V_4 - z)c + (V_5 - z)c}{4}} \quad (13)$$

Since c is in every term, it is possible to cancel it out.

$$C_{P_{Total}} = \frac{(V_1 - z) - (V_T - z)}{(V_1 - z) - \frac{(V_2 - z) + (V_3 - z) + (V_4 - z) + (V_5 - z)}{4}} \quad (14)$$

The z term in the numerator cancels out, while the z term in the denominator can be simplified

$$C_{P_{Total}} = \frac{V_1 - V_T}{(V_1 - z) - \frac{V_2 + V_3 + V_4 + V_5 - 4z}{4}} \quad (15)$$

Finally, the z term in the denominator cancels out.

$$C_{P_{Total}} = \frac{V_1 - V_T}{V_1 - \frac{V_2 + V_3 + V_4 + V_5}{4}} \quad (16)$$

Equation 16 shows that when calculating $C_{P_{Total}}$, or for that matter any of the C_P values, the zeros and calibration factors cancel each other out. Thus, using only one transducer eliminates the source of error that could be caused by miscalibration of a transducer.

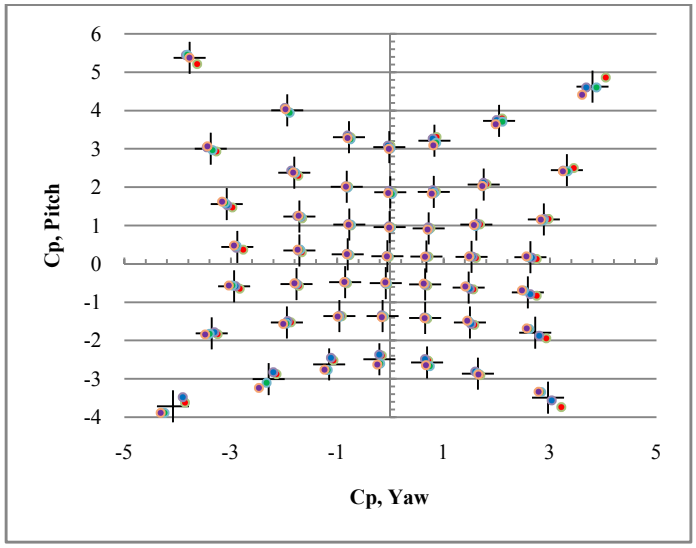

Figure 8: Average Values with Measured Points Re≈2650

In Figure 8, the center of the symbols (crosses) represents the average value, while the four points surrounding each cross represents the data individually collected from each run. Nearly all points within the ±20° range are very close to the average value. It is on the outlying areas, those greater than ±20°, that the blocks start to get bigger and small errors, such as a misalignment start to become more pronounced. The star formed carpet map as shown in Figure 8 is not perfectly symmetrical because a dimensionally perfect and symmetrical

five-hole probe is very difficult to obtain during the even the best hand manufacturing process used.

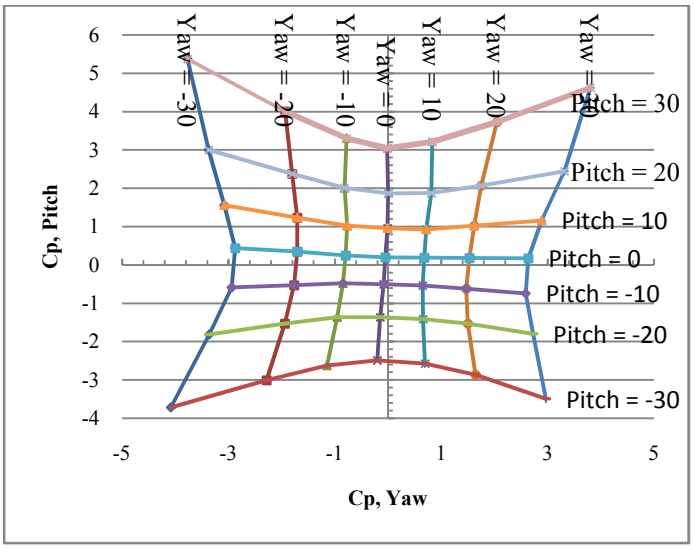

Figure 9: Average Value Calibration Map Re≈2650

Figure 9 shows a typical averaged carpet map produced by our current automated approach. This map is used for finding the pitch and yaw angles during a five-hole probe measurement.

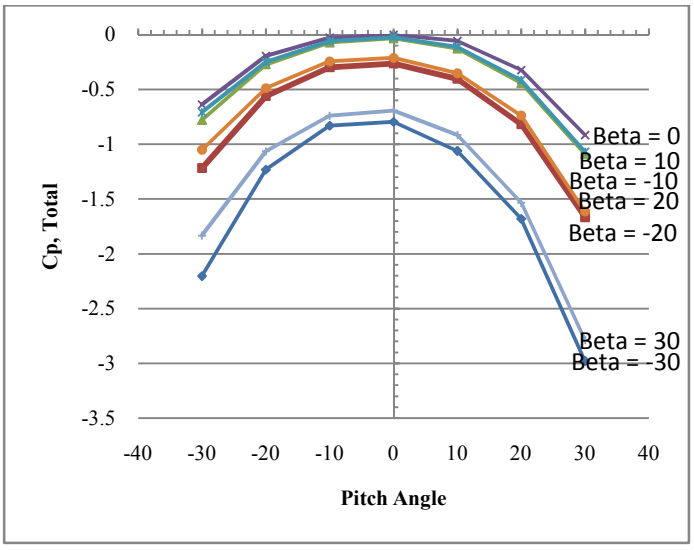

Figure 10: Average Value $C_{p,\,Total}$ Calibration Map Re≈2650

Figure 10 shows the variation of total pressure coefficient $C_{p_{total}}$ with respect to pitch and yaw angle. Total pressure coefficient can be obtained from Figure 10 by using the pitch and yaw angle deduced from Figure 9.

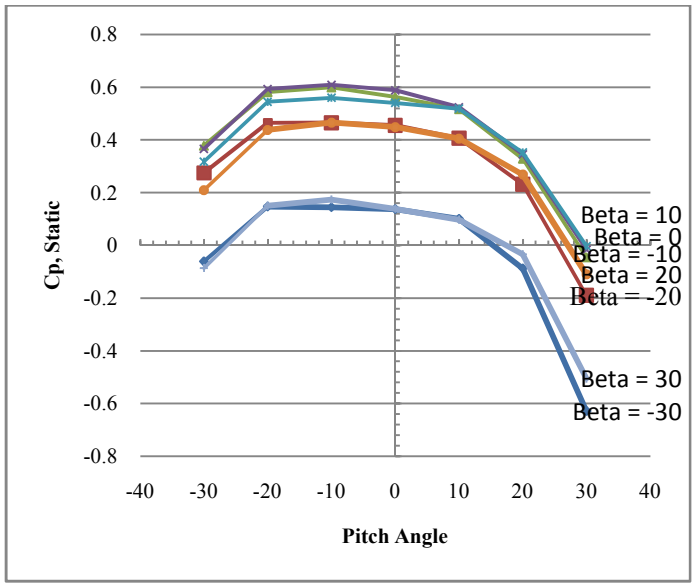

Figure 11: Average Value $C_{p,\,Static}$ Calibration Map Re≈2650

Figure 11 provides the static pressure coefficient $C_{p_{static}}$ as a function of pitch and yaw angle. Local static pressure from the five-hole probe measurement can easily be recovered from Figure 11 after determining the pitch and yaw angle.

Improved Repeatability

One of the major advantages of the current computer automated system over doing these calibrations by hand is the repeatability of computer driven pitch and yaw angle adjustments. The computer calculates the movements based on user-defined range and outputs the number of steps. It then moves the mechanisms shown in Figure 5 and Figure 6 to their proper location. The computer driven stepping motor controller can move the stepping motor shaft 0.025° for each stepper pulse issued. For a 1° change in the pitch or yaw angle, typically 40 steps from the motor controller are needed. Once the initial zero pitch and yaw position are adjusted, the computer driven mechanism can move to a new position with excellent spatial resolution and accuracy.

Time reduction

Calibration of five-hole probes by manual pitch and yaw angle adjustments is a very long and arduous project. Previously, a 49-point map in a manual calibration effort took at least three hours to complete since a high quality manual adjustment of each pitch and yaw angle required great care. With the original rig, time to run the complete calibration for a 49-point map took 75 minutes. When the design was changed to the improved one as shown in Figure 6, and thus the rotary tables switched their yaw and pitch assignments, the amount of time to run the calibration was reduced to 65 minutes. This is because the pitch motor is now the B4800TS, and it takes a slightly larger step than the B5990TS. Since the program was written so that the pitch angle is moved more often than the

yaw angle, the reduction in the number of steps needed to change the pitch angle resulted in a shorter calibration time. Ensemble averaging from four individually obtained carpet maps can also be very easily obtained in the current computer driven system, in a time efficient manner. Averaging is an excellent way of removing some of the error originating from the initial zero pitch/zero yaw alignment of the probe before each calibration sequence.

New Design

The method of initial attachment of a five-hole probe to a pitch and yaw calibrator is extremely critical mainly because the style and quality of mechanical attachment influences the movement of the probe tip. Attaching the probe as shown in Figure 5 results in large swings and displacements of the probe tip. This approach may introduce large errors at calibration wind tunnel test sections where spatial uniformity is not at an acceptable level. Figure 6 showed a much-improved design where the probe's bend is located at the intersection of the two rotational axes. The probe tip in the improved design did not change its position as much as it did with the original mechanism as shown in Figure 5. The improved design shown in Figure 6 not only saved time, but it also made the map more accurate.

Alignment

Due to the nature of the manufacturing of the probe, the initial alignment must be performed by hand. This is because of its small size, and unseen manufacturing defects that make nulling the probe unfeasible. However, a few techniques were developed in order to increase the accuracy. First, a "plummet" was used to create a line directly below the exit of the wind tunnel. This line was used to set the bottom of the calibrator parallel to the exit of the wind tunnel. This helped insure that the probe was correctly aligned for the pitch calibration.

The yaw calibration was done with the help of a visible laser beam. By using a tripod and a piece of paper over the exit of the wind tunnel it was possible to compare the shape of the shadow of the probe. The shadow was then brought to its minimum size by making small adjustments with the yaw stepper motor. The previous two alignments were done at the beginning of every run.

Uncertainty Estimates

An uncertainty analysis was prepared for the total pressure, the static pressure, and the velocity found in Equation 6, Equation 7, and Equation 8 respectively. An adaptation of a method set forth by Taylor [13] was used. The following gives an example using the total pressure calculations.

$$\delta P_T = \left(\left(\delta P_1 \frac{\delta P_T}{\delta P_1} \right)^2 + \left(\delta P_2 \frac{\delta P_T}{\delta P_2} \right)^2 + \left(\delta P_3 \frac{\delta P_T}{\delta P_3} \right)^2 + \left(\delta P_4 \frac{\delta P_T}{\delta P_4} \right)^2 + \left(\delta P_5 \frac{\delta P_T}{\delta P_5} \right)^2 + \left(\delta C_{P_{Total}} \frac{\delta P_T}{\delta C_{P_{Total}}} \right)^2 \right)^{1/2} \qquad (17)$$

Equation 17 is the general form used to find the uncertainty of the total pressure measurement. First, the accuracy of the transducer was found to be approximately 3.5 Pa. Due to the additional equipment and high L/D tubing, this number was increased to five Pascals. This is expressed in Equation 18.

$$\delta P_1 = \delta P_2 = \delta P_3 = \delta P_4 = \delta P_5 = \pm 5\ Pa \qquad (18)$$

Next, the accuracy of the total coefficient of pressure had to be estimated. This was found by subtracting the minimum from the maximum of the measured calculated values from all runs and dividing it by two. This caused the measurements to be more closely grouped together near the center point and have larger errors near the edges.

$$\delta C_{P_{Total}} = \pm {}^1/_2 \left(C_{P_{Total\,Max}} - C_{P_{Total\,Min}} \right) \qquad (19)$$

Finally, the partial differentials in Equation 17 were calculated. The differentials using pressures came out to be unitless, while the differential using the coefficient of pressure came out to be in Pa.

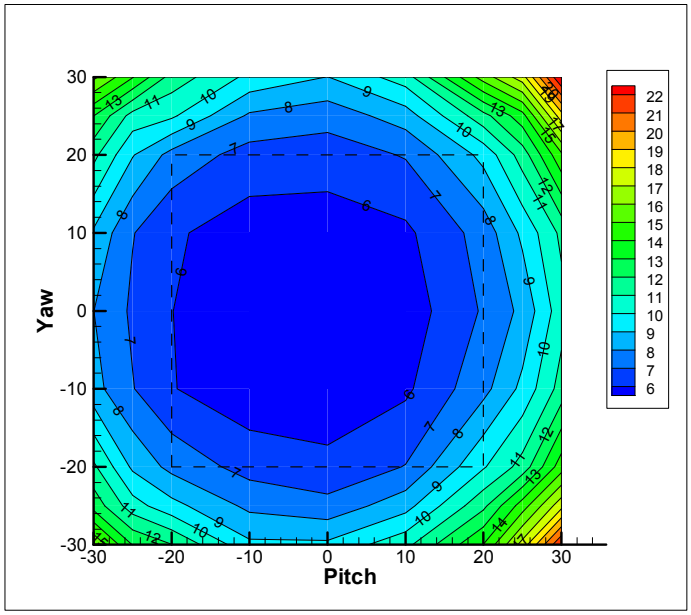

Figure 12: ±Total Pressure Error at Re≈2650 (Pascal)

Figure 12 shows the total pressure error in terms of a ± Pascal range. Here the most accurate part of the probe is located slightly left of the zero pitch zero yaw location. This is most likely due to small defects (asymmetries in the probe tip shape) in the probe. The dashed box in the figure represents the ±20° range. This box is to help identify the central range for which the probe is accurate.

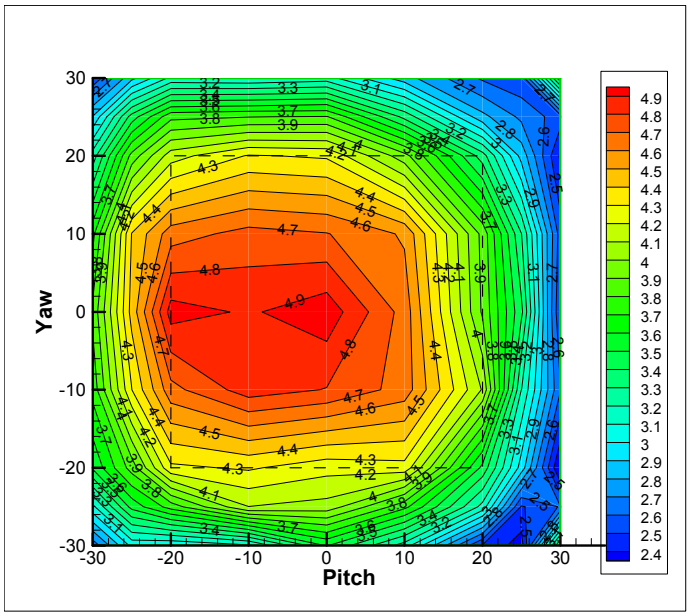

Figure 13: ±Static Pressure Error at Re≈2650 (Pascal)

Figure 13 represents the static pressure error. Once again the error is slightly offset from the center point due to imperfections. The error near the center of the probe is larger than the error near the edges. This is most likely because of the way that the static pressure is calculated. When the probe is aligned with the flow, the values at each of the probe points increase in magnitude. This also increases the amount of uncertainty they produce. While on the edge, the pressure at some of the points decease and the overall uncertainty is reduced.

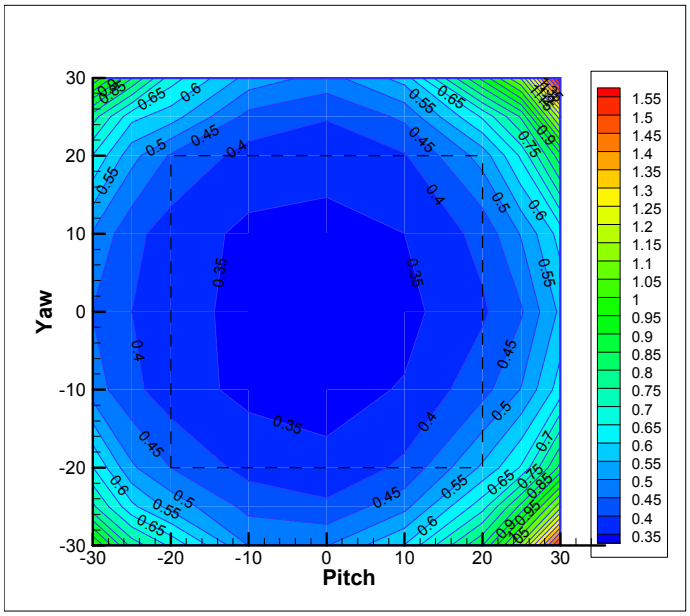

Figure 14: ±Velocity Error at Re≈2650 (m/s)

Figure 14 is shows the velocity error. Here the area of minimum error is in the center. It grows as we move away and reaches a maximum at the corners.

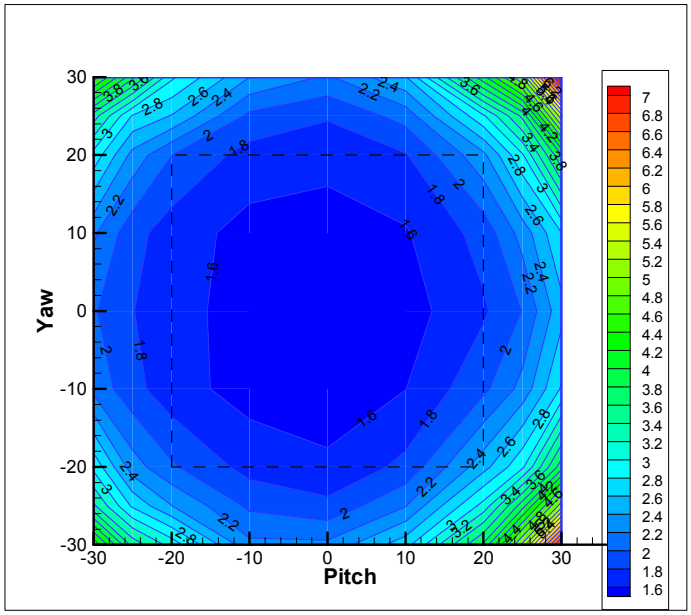

Figure 15: Velocity Error Percent at Re≈2650 (Local Error Divided by Wind Tunnel Velocity)

Figure 15 represents the velocity error of Figure 14 divided by the velocity of the wind tunnel (22.2 m/s). The smallest percent of error is located at the center of the map, while the largest are near the edges. The dashed box marks the ±20° range. Within this range, there is no percent error over 2.4%. The estimated velocity error within ±10° range is about 1.6% of the calibration tunnel velocity.

From the preceding figures, it was determined that the ideal operation of this probe would be within the ±20° range that was defined with the dashed box. The pitch and yaw range of the ±30° is also possible. However, the elevated measurement errors should be carefully evaluated in this range of operation.

CONCLUSIONS

Using the computer in the calibration of a five-hole probe has made the overall calibration sequence quicker to produce the calibration maps, and as such, it is possible to produce multiple maps for further ensemble averaging purposes. This allows for an average to be taken and an increase in the accuracy. The use of one transducer also resulted in an increase in accuracy by eliminating some of the zero and calibration errors. It is also possible to increase the resolution of the map in order to help quantify the non-linear parts located near the corners of the carpet map. Such a system can also easily be adapted to other types of probes that also need to be calibrated at varying pitch and yaw angles. The improved calibration mechanism using a computer driven pitch and yaw calibrator resulted in a velocity

error of 1.6% of the calibration tunnel test section velocity within the ±10° pitch and yaw angles. The error is about 2.4% when the pitch and yaw range is enlarged to ±20°.

ACKNOWLEDGMENTS

The authors would also like acknowledge H. E. Houtz for the fabrication of the five-hole probe and the assembly of the pitch and yaw mechanism. Acknowledgments are also due to Dr. Ali Akturk and Ozhan Turgut for their continuous interest and support throughout this effort.

REFERENCES

[1] Wiedner, B.G., 1994, "Passage Flow Structure and its Influence on Endwall Heat Transfer in a 90° Turning Duct" Ph.D. Thesis, Pennsylvania State University, University Park, PA.

[2] Treaster, A.L., and Yocum, A. M., 1979, "The Calibration and Application of Five-Hole Probes," ISA Transactions, **18**(3), pp. 23-34.

[3] Ostowari, C., and Wentz, W. H., 1983, "Modified Calibration Techniques of a Five-Hole Probe for High Flow Angles," Experiments in Fluids, **I**(3), pp. 166-168.

[4] Nowack, C. F. R., 1970, "Improved Calibration Method for a Five-Hole Spherical Pitot Probe," Journal of Physics E: Scientific Instruments, (1), pp. 21-26.

[5] Weiz, J. P., 1980, "An Algorithm for Using the Five-Hole Probe in the Non-nulled Mode," The Applied Research Laboratory of the Pennsylvania State University, University Park, PA.

[6] Reichert, B. A., and Wendt, B. J., 1994, "A New Algorithm for Five-Hole Probe Calibration, Data Reduction, and Uncertainty Analysis," NASA, Lewis Research Center, Internal Fluid Mechanics Division, Cleveland, OH.

[7] Dominy, R. G., and Hodson, H. P., 1993, "An Investigation of Factors Influencing the Calibration of Five-Hole Probes for Three-Dimensional Flow Measurements," Journal of Turbomachinery, (115), pp. 513-519.

[8] Morrison, G. L., Schobeiri, M. T., and Pappu, K. R., 1998, "Five-hole Pressure Probe Analysis Technique," Flow Measurement and Instrumentation, (9), pp. 153-158.

[9] Lee, S. W., and Yoon, T. J., 1999, "An Investigation of Wall-Proximity Effect Using a Typical Large-Scale Five-Hole Probe," Korean Society of Mechanical Engineers International Journal, **13**(3), pp. 273-285.

[10] Brophy, M. C., Treaster, A. L., Stinebring, D. R., and Weiz, J. P., 1980, "Optimization of a Five-Hole Probe Wake Measuring System," Technical Memorandum 87-156, The Pennsylvania State University, State College, PA.

[11] Sitaram, N., Lakshminarayana, B., and Ravindranath, A., 1980, "Conventional Probes for the Relative Flow Measurement in a Rotor Blade Passage," ASME Paper No.A80-36126 14-35, *Proceedings of the Joint Fluids Engineering Gas Turbine Conference and Products Show, New Orleans, LA, March 10-13, 1980, American* Society of Mechanical Engineers, New York.

[12] Treaster, A. L., and Houtz, H. E., 1986, "Fabricating and Calibrating Five-Hole Probes," ASME Paper No. A86-40704,*Proceedings of the Fourth Fluid Mechanics, Plasma Dynamics, and Lasers Conference, Atlanta, GA, May 11-14 1986,*American Society of Mechanical Engineers, New York.

[13] Taylor, J. R., 1997, *An Introduction to Error Analysis the Study of Uncertainties in Physical Measurements*, University Science Books, Sausalito, CA, pp. 75, Chap. 3.

[14] Ligrani, P. M., Singer, B. A., and Baun, L. R., 1989, "Miniature Five-hole Pressure Probe for Measurement of Three mean Velocity Components in Low-speed Flows," Journal of Physics E: Scientific Instruments, **22**(10), 868-876.

